DOI: 10.31276/VJSTE.66(2).10-18

Convective heat transfer by nanofluid jet impingement cooling on automobile radiator with nozzle plate spacing

M. Peeraiah[1*], K. Nagamalleswara Rao[2], B. Balakrishna[3]

[1]Department of Mechanical Engineering, JNTU College of Engineering, Kakinada, Andhra Pradesh, India
[2]Department of Mechanical Engineering, Velagapudi Ramakrishna Siddhartha Engineering College, Vijayawada, Andhra Pradesh, India
[3]Department of Mechanical Engineering, JNTU College of Engineering, Kakinada, Andhra Pradesh, India

Received 3 October 2023; revised 20 November 2023; accepted 3 May 2024

Abstract:

Nanofluids are a type of emerging heat transfer fluid with great promise for thermal engineering due to its high heat transfer coefficients. Improving heat transmission remains an ongoing task in engineering fields as diverse as semiconductor technology and high-performance vehicles. This paper investigates and compares the jet impact heat transfer coefficient, thermal conductivity, and viscosity of nanofluids with those of a base fluid in an automobile radiator with nozzle plate spacing. Aluminium oxide (Al_2O_3) and deionised water were selected as the working fluids, and they were used in varying quantities ranging from 0 to 1 volume percent. The nanofluids were prepared using a two-step method with the aid of an ultrasonic homogeniser. The results reveal that the heat transfer coefficient increased by 11.68% at a nanofluid concentration of 1% when nanoparticles were suspended in the base fluid. Furthermore, a 45-49% improvement in the heat transfer coefficient was recorded using a nanoparticle volume concentration of 1% compared to the base fluid.

Keywords: **heat transfer coefficient, jet impingement, volume concentration.**

Classification numbers: **2.1, 2.3**

1. Introduction

Enhancing heat transport is pivotal in heat transfer engineering, with a pressing need to boost the efficiency of thermal devices in various technical fields [1]. Strategies such as increasing the heat transfer area and coefficient have been explored extensively [2]. However, technological advancements in heat transmission have reached their limits. Recent research has shown that incorporating nano-sized nanoparticles into liquids can significantly increase the heat transfer coefficient compared to conventional liquids [3]. This led to the development of "nanofluid", where particles sized 1 to 100 nm are suspended, markedly improving heat transfer [4]. Subsequent studies have focused on the heat transfer coefficients of various nanofluids.

A. Kumar, et al. (2020) [5] noted an 18% improvement in heat transfer with a 4% volume concentration of copper and copper oxide nanoparticles. A. Banisharif, et al. (2020) [6] found that thermal conductivity of nanofluids increases exponentially with nanoparticle volume concentration. Viscosity, critical for evaluating a material's heating capacity, influences the pressure drop and thus the transport power, making its reduction crucial to increasing heat transmission [7]. According to experimental research conducted in [8], the viscosity of an Al_2O_3-DI water nanofluid substantially increases. At a concentration of 5% volume, the viscosity of an Al_2O_3-DI water nanofluid rises significantly, with a 79% increase at a 5% volume concentration [9].

Another vital aspect of nanofluids is their density, which affects the fluid pressure drop along with viscosity. The nanofluid density does not depend on characteristics such as nanoparticle size, shape, and additives; instead, density primarily depends on the nanoparticle material [10]. The viscosity of nanofluid is shown to rise with increasing nanoparticle concentration since solids have a more significant density than liquids [11]. There is a pressing need for more literature on the topic of nanofluid density.

The specific heat (C_p) of nanofluids is another essential property that determines the nanofluid's thermal ability to conserve energy. Nanofluid C_p is determined by several distinct criteria, including the type, volume concentration of particles, and the base fluids, evaluated at various temperatures [12]. R.S. Vajjha, et al. (2010) [13] were the first to show that particle volume concentration increases in nanofluids containing aluminium oxide/titanium oxide/

*Corresponding author: Email: shreepeeru@gmail.com

water while the C_p of the nanofluids decreases. J.R. Satti, et al. (2016) [14] researched the specific heat of nanofluids containing aluminium, silicon, and zinc oxide nanoparticles. They also found that the specific heat drops with increasing nanoparticle concentration but rises with nanofluid temperature.

Experiments with alumina-water nanofluids at varying nanoparticle concentrations were previously published [15], which determined particle concentration improved the heat transfer coefficient of the heat transfer of H_2O and 0.4 vol.%. TiO_2 nanoparticles in a parallel flow exchanger under uniform flow conditions [16]. The mass flow rate of the nanofluid and water, as well as the temperature of the nanofluid, were shown to affect the heat transfer coefficient significantly. Nanofluids were shown to have a 16% greater heat transfer coefficient than the primary liquid.

The heat transfer coefficient of aluminium oxide-water nanofluids was studied in a flow with a horizontal heated tube [17]. When combined with water, the aluminium oxide-water nanofluid at 6 vol.% boosted heat transfer at entry and in fully formed regions by 13 and 24%, respectively. Heat transfer properties of TiO_2/Al_2O_3-water nanofluids were studied in [18, 19] in a heat exchanger with turbulent flow. They found that a 0.5% volume concentration of Al_2O_3/water nanofluids resulted in a maximum improvement of the total heat transfer coefficient by roughly 27%. At a particle volume concentration of 0.4%, TiO_2/water nanofluids showed the most significant improvement.

S. Jena, et al. (2020) [20] looked at the metal oxide nanoparticles in oil using scientific methods to improve heat transfer. The results showed that as the nanoparticle volume concentration increases, so does the temperature of the fluid. P.K. Pattnaik, et al. (2021) [21] studied how a micropolar liquid that conducts electricity moves freely over a surface that is being stretched. It shows and discusses how characterising factors affect the flow phenomenon. No matter how much the slip number increases, the data shows an apparent slowing down in the velocity curves due to more drag. S.K. Parida, et al. (2021) [22] investigated the effect of dust particles on nanofluid flow due to the interaction of thermal radiation parameters. The authors discovered that the nanoparticle's volume percentage and radiative energy favour increasing rates of energy transfer near the sheet's surface.

P.K. Pattnaik, et al. (2022a) [23] examined the 2D flow of water-based nanofluids and used a fluid with pores to show how a longitudinal magnetic field works. The nanofluid is made by mixing copper and aluminium oxide nanoparticles with carbon nanotubes in water, the base fluid. The findings showed that as the particle concentration goes up, the shear rate coefficient does as well, while the heat transfer rate decreases. P. Mathur, et al. (2021) [24] studied second-order velocity slip by moving a nanofluid past a stretched surface. The work describes how several factors that define the flow behave in different situations. The results show that the fluid's velocity slows as the material value increases. P.K. Pattnaik, et al. (2022b) [25] studies how floating forces affect the flow of a conducting nanofluid via hollow walls that change over time. It also looks at the heat absorption factors that affect the nanofluid model. The results show that adding volume fractions makes them move faster near the channel's inner layer and slower near its porous walls.

For their study, P.C. Pattanaik, et al. (2022) [26] examined the Newtonian flow properties of the nanofluid using a parallel path because of thermal stability. As the particle volume concentration goes up, the fluid motion slows down. However, the slowing down of the water-based nanofluid is greater than that of the oil-based nanofluid. B. Mohanty, et al. (2021) [27] put an electrically conductive nanofluid in a curved tube and let it connect to radiated heat energy and a heat sink. The lower alpha potentials show Joule heating also affects the flow processes. The results showed that the Newtonian fluid significantly affects the fluid properties, even if the parameter is visible. S.R. Mishra, et al. (2019) [28] investigated how heat transfer affects a hybrid fluid's flow along an endless flat surface with radiation. The regular electromagnetic field was put in place along the primary flow direction. The results show that the velocity profile got faster when adding the parameter, but the border layer got thinner when the inertia effects were added.

S. Baag, et al. (2018) [29] investigated how heat moves through a thermal boundary layer that flows over a stretched sheet in a steady heat source. The work showed that the force slows down the velocity profile everywhere in the velocity boundary layer. B. Nayak, et al. (2019) [30] studied the flow over a porous rectangular surface with chemical processes rather than heat transmission. The results show that as the number of heavy species increases the reaction time, the quantity of liquid in its boundary region decreases. O.D. Makinde, et al. (2017) [31] examined the gravity forces and changing viscosity affected the mixed flow of a conducting fluid over a porous plate that was heated by convection. It has been found that when an electromagnetic field is present, skin friction decreases, the Reynolds number increases, and the fluid's viscosity decreases.

K.S. Nisar, et al. (2021) [32] investigated the nanofluid flow over an expanded surface that was open, turbulent, and could not be compressed. A steady source of heat and chemical process also improves the heat transfer qualities

of a nanofluid. The results show that raising the fluid concentration lowers the temperature of the fluid when the Nusselt number is high. S. Mishra, et al. (2022) [33] studied the nanofluids using a solid-state reaction process at high rates and pure start ingredients such as tungsten trioxide. The results reveal that the primary crystal structure size is 38 mm, and strains are 0.11%. In their study, S. Mishra, et al. (2021) [34] investigated the radiant flow of a bipolar nanofluid over a flexible film. They looked at the effects of heat flux. The findings show that increasing the radiation and heat production factors improves the temperature distribution.

Automobiles require several vital components, including radiators. The engines are cooled by a heat exchanger system, which is one such system. Like other thermal devices, the engine presents a significant challenge in thermal management. It improves engine efficiency by increasing the heat transfer capacity of the radish radiators. In the radiator of an automobile, water has often been used instead of other coolants. The performance of automobile radiators can be improved with the recent commercial introduction of 50:50 mixes of ethylene glycol and water [35]. Using nanofluid may enhance the heat transfer efficiency of heat exchangers. However, thermal conductivity, viscosity, and density must first be investigated since the efficiency of the automobile radiator is reliant on these parameters before the heat transfer efficiency can be studied. Only a little amount of research has been done on the viscosity of a nanofluid based on radiator coolant.

The current study examines the heat transfer coefficient, thermal conductivity, and viscosity of nanofluids based on a radiator coolant containing aluminium oxide nanofluids at temperatures varying from 0 to 60˚C. Filling the gaps in understanding the fundamental thermophysical characteristics of nanofluids based on radiator coolants is the goal of this study.

2. Preparation of nanofluids

Two-step method for preparation of nanofluids is presented in Fig. 1.

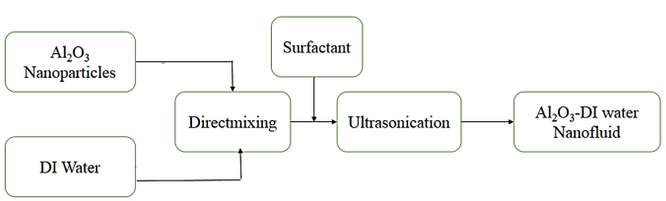

Fig. 1. Two-step method for preparation of nanofluids.

Aluminium oxide nanoparticles were purchased from Sigma-Aldrich Chemicals Ltd. and combined with coolant at a volumetric concentration of 0 to 1% vol.% with a particle size of 20 nm according to the following formula:

$$\text{Volume concentration } (Ø) = \frac{\frac{m_n}{\rho_n}}{\frac{m_n}{\rho_n}+\frac{m_f}{\rho_f}} \quad (1)$$

where *m* denotes the mass and ρ denotes the concentration of the nanoparticles and coolant; n denotes nano, f denotes fluid. Thus, 100 g of the base fluid was used to make the nanofluid samples, and then the predicted amount of Al_2O_3 was added to the liquid itself. To attain uniform dispersion in the base fluid, the nanoparticle solution was maintained in a sonicator, a mechanical stirrer, and stirred continuously for around 6 hours. The nanoparticles were dissolved in the base fluid, and the surfactant was added to create the nanofluids. According to the formulae for the solid-fluid mixtures, the properties of the nanofluids were assessed. The thermophysical characteristics of Al_2O_3, the base fluid (DI water), and air at 30˚C are listed in Table 1.

Table 1. Properties of the nanofluids.

Fluid	Density (Kg/m³)	Viscosity (Pas)	Specific heat (kJ/kg K)	Thermal conductivity (W/mK)
Al_2O_3 nanoparticles	3970	22	765	36
DI water	997	10^{-3}	4184	0.6

The density [36], viscosity [37], and thermal conductivity [38] were calculated using the following equations:

$$\rho_{nf} = Ø\rho_p + (1 - Ø)\rho_{bf} \quad (2)$$

$$\mu_{nf} = A\left(\frac{1}{T}\right) - B \quad (3)$$

$$A = 20587Ø^2 + 15857Ø + 1078.3$$

$$B = -107.12Ø^2 + 53.54Ø + 2.8715$$

$$K = \frac{k\rho + (n-1)K_f - 2(n-1)Ø(K_f - K_p)}{K_p + 2K_f - (K_f - K_p)} K_f \quad (4)$$

2.1. SEM analysis

Scanning electron microscope imaging was used to examine the surface structure of the Al_2O_3 nanoparticles. Images of pure Al_2O_3 nanoparticles are shown as samples in Fig. 2. As seen in the figure, Al_2O_3 nanoparticles are very twisted tubes with a 20 nm diameter.

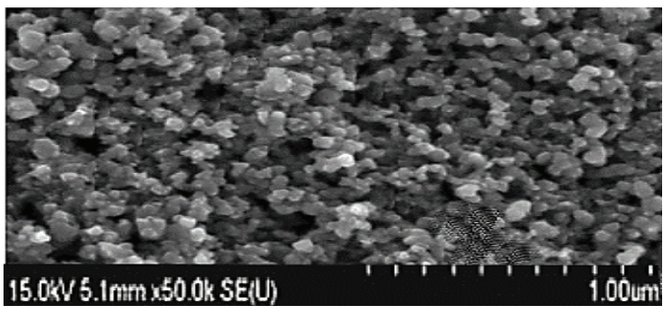

Fig. 2. SEM image of the Al_2O_3 nanoparticles.

2.2. X-Ray diffraction analysis

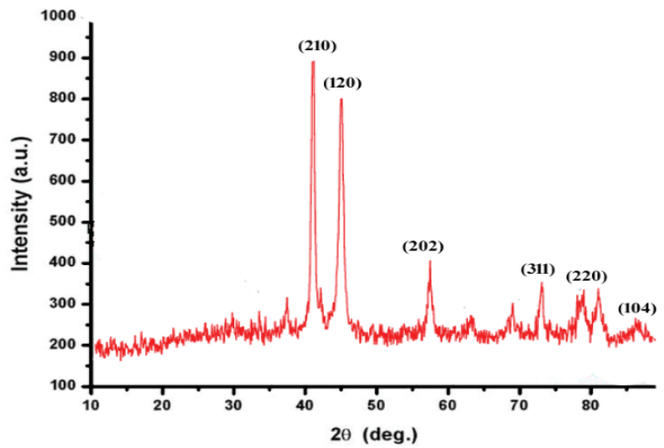

Fig. 3. XRD of the Al_2O_3 nanoparticles.

The size and structure of Al_2O_3 nanofluids are characterised using X-ray diffraction analysis (Fig. 3). Six peaks at 30˚C are seen in the XRD pattern shown in Fig. 3, identical to the (210), (120), (202), (311), (220), and (104) orientations. The optimal alteration of Al_2O_3 nanoparticles is demonstrated by a shift in the location of the distinctive peak in the pattern produced by XRD. Further evidence that Al_2O_3 nanoparticles have preserved their initial form after functioning comes from the lack of a dramatic shift in the location of distinctive peaks. This is evidence that the acid-functionalised Al_2O_3 nanoparticles have an ordered flow of structure. Due to the chemical treatment performed throughout the experiment, Al_2O_3 nanoparticles were functionalised with carboxylic groups, increasing their reactivity. These results show that the Al_2O_3 nanoparticles were tightly adhered to the surface due to this functionalisation.

3. Experimental arrangement

The schematic of the experimental setup is presented in Fig. 4.

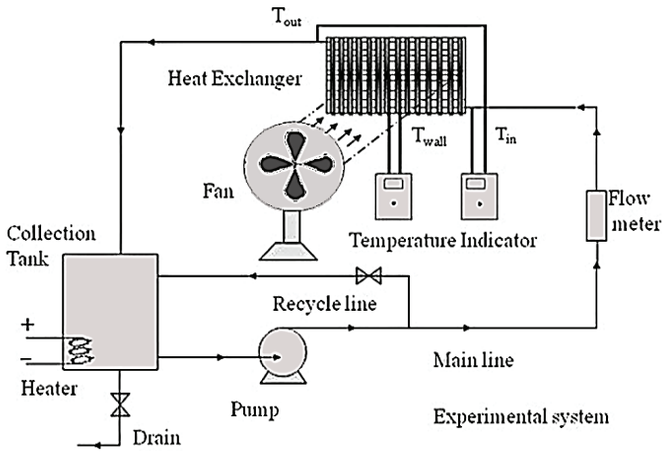

Fig. 4. Schematic of the experimental setup.

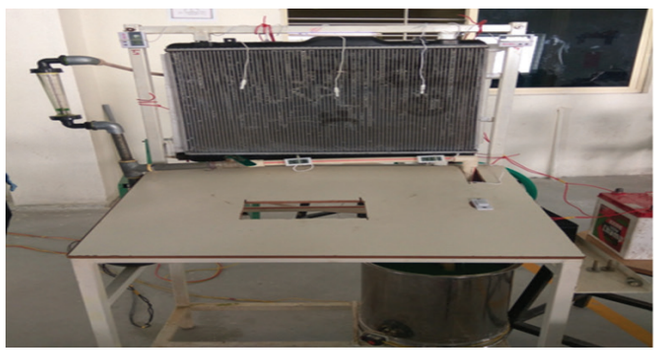

Fig. 5. Image of the experimental setup.

Figure 5 depicts the evaluation of the intended test rig with a conduit attached. The coolant in the container is brought up to the appropriate temperature, and then the pump is activated, allowing the coolant to circulate through the radiator. Finally, the fan is activated to blow air over the radiator, which removes heat from the radiator. Temperatures are recorded at the radiator's intake and output. It is anticipated that the nanofluid will flow with a constant Reynolds number and will be able to tolerate average circulation in the radiator. The coolant circulates via 104 tubes, each 5 mm wide and 0.3 m long. Using a rotameter, it is estimated that the coolant can flow through the radiator at flow rates of 3, 6, 9, and 12 litres per minute. Changing the coolant and air flow rates is necessary to replicate realistic working conditions in an administrative setting. The temperatures of the air entering and exiting the radiator are both measured.

When the desired temperature is reached, the heat exchanger's coolant pump is turned on to circulate high-temperature, durable coolant through the unit. The radiator's coolant entry and exit temperatures are measured using T-type thermocouples. A set of thermocouples measures the

air temperature affixed to the front and rear radiator tubes at various points. Experiments are run with a perforated plate at distances of 10 and 15 cm from the radiator to test the effect of varying L/D ratios. Fig. 6 shows a side view of the test rig, which includes temperature thermocouples for the coolant and air inlets and outlets. Photographs of the nozzle sheet arrangement, which is located between the fan and the radiator, are shown in Fig. 7.

Fig. 6. Side view of the experimental setup.

Fig. 7. Images of nozzle arrangement plate with a diameter of 30 mm.

3.1. Estimation of heat transfer coefficient

The formulae below were used to determine the heat flow rate and flow rate of the air passing through the fins to the radiator:

$$Q = hA(T_b - T_w) \quad (5)$$

The heat transfer can be calculated as follows:

$$Q = mC_p\Delta T = mC_p(T_{in} - T_{out}) \quad (6)$$

$$N_u = \frac{h_{exp}\, d_h}{K} = \frac{m_{Cp}(T_{in}-T_{out})}{A\,(T_b-T_w)} \quad (7)$$

Nomenclature

Cp: specific heat; D: diameter; K: thermal conductivity; m_n: Mass of nanoparticle; N_u: Nusselt number; T: temperature.

Subscripts

Bf: base fluid; f: fluid; h: hydraulic; in: inlet; nf: nanofluid; out: outlet; p: particle.

Greek symbols

Ø: volume fraction; ρ: density.

4. Results and discussion

4.1. Effect of heat transfer coefficient

Figure 8 shows the dependence of the total heat transfer coefficient on the nanofluid flow rate for a range of nanofluid volume concentrations. As observed, increasing the nanofluid flow rate significantly raises the nanofluid's total heat transfer coefficient. When comparing the base fluid to the nanofluid, the total heat transfer coefficient increases as the nanoparticle concentration increases. At a nanoparticle concentration of 1 vol.%, the total heat transfer coefficient of Al_2O_3/DI water nanofluids is increased by 12% compared to the base fluid [39]. At a concentration of 0.8 vol.%, the nf improves the total heat transfer coefficient by 9%. The increase in heat transfer coefficient using nf may be described by the heat transfer simulation, the reduction in thermal boundary layer thickness, and an increase in thermal conductivity. Furthermore, the significant reason for this improvement in thermal conductivity of nf in the radiator pipe flow [40]. This represents the inconsistent particle concentration in the tubes.

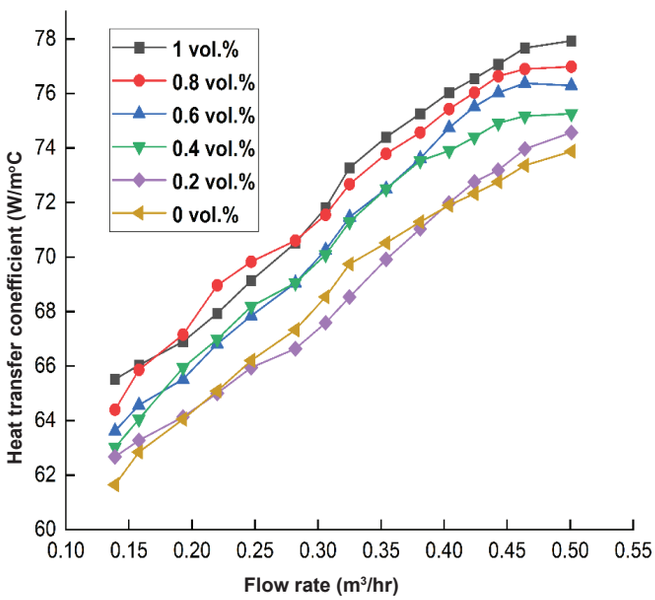

Fig. 8. Variation in nanofluid flow rate as a function of concentration and heat transfer coefficient.

4.2. Effect of thermal conductivity

Figure 9 shows the temperature-dependent thermal conductivity of aluminium oxide-radiator coolant nanofluid at varying volume concentrations. The illustration demonstrates that the nanofluid's thermal conductivity increases as both concentration and temperature rise. The thermal conductivity of both the base fluid and the nanofluid

increases with temperature, but the nanofluids exhibit better thermal conductivity than the base fluid at all concentrations due to the motion of particles during heating. As the fluid's temperature rises, the particles move more rapidly against one another, increasing the fluid's thermal conductivity.

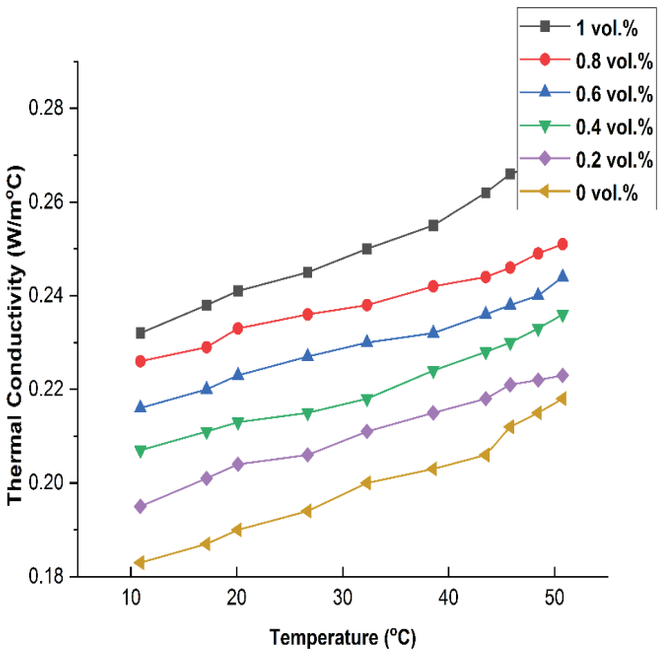

Fig. 9. Changes in nanofluid thermal conductivity with temperature.

The thermal conductivity of the base fluid was 0.250 W/mK at 10°C, whereas that of the nanofluid was 0.270 W/mK with a concentration of 1 vol.%, an increase of 8%. This indicates that the nanofluid's thermal conductivity improves as its concentration rises. At 50°C, the thermal conductivity of the base fluid and the nanofluid at 1 vol.% were 0.259 and 0.280 W/mK, respectively [41]. At a concentration of 1 vol.%, the thermal conductivity of the nanofluid is 8.30% higher than that of the base fluid at the same temperature. In every instance, the nanofluid was shown to have superior thermal conductivity than the base fluid. The thermal conductivity of nf has been observed to increase almost linearly. However, the lines on the graph do not match up perfectly. The nanofluid's thermal conductivity may be affected by factors other than particle concentration and temperature, such as particle size and shape.

Radiator coolant-based nanofluids experimental data on their thermal conductivity are shown in Fig. 10. This data compares the thermal conductivity values of Al_2O_3-radiator cooled nanofluid at 27°C with several empirical models at various volume concentrations ranging from 0 to 1% [42, 43]. Both experiments and established models show that as concentration increases, so does thermal conductivity. However, when using an Al_2O_3-based radiator coolant, the thermal conductivity model of R.L. Hamilton, et al. (1962) [43] is 1.92% higher than that of N. Kumar, et al. (2018) [42]. The experimentally determined thermal conductivities for a 1 vol.% concentration of Al_2O_3-based nanofluid were 4.26 and 2.20% higher than the estimated thermal conductivities using the N. Kumar, et al. (2018) [42] and R.L. Hamilton, et al. (1962) [43].

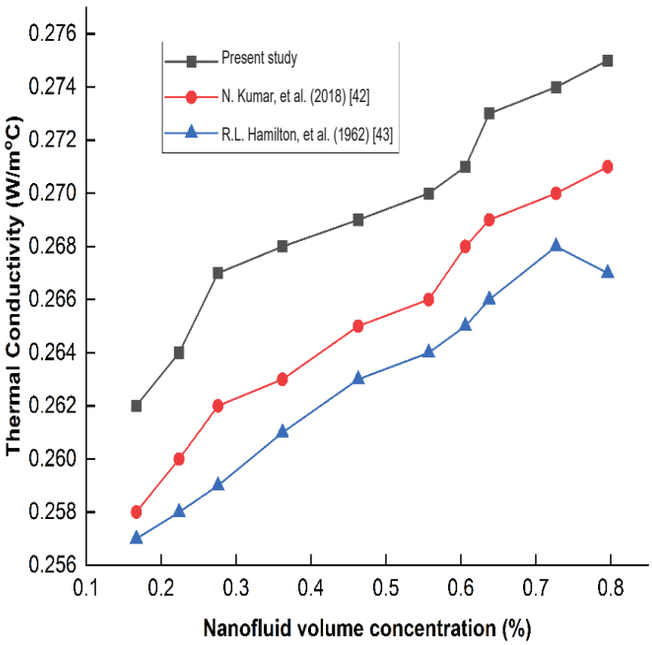

Fig. 10. Comparison of the experimental data with models.

4.3. Effect of viscosity

From 10 to 50°C, and at 0 to 1 vol.% nanoparticle concentration, the viscosities of Al_2O_3-DI water-based nanofluid were measured. Fig. 11 demonstrates that as the temperature increases, nanofluid viscosity decreases rapidly. The nanofluid has a higher viscosity at all volume concentrations than the base fluid. Moreover, the viscosity of the nanofluid is shown to rise with the concentration in the base fluid and to decrease with an increase in temperature. The viscosity of the nanofluid falls by 61.05% when raised from 10 to 50°C, whereas the viscosity of the base fluid decreases by 72.11% over the same temperature range. In general, liquids tend to become less dense as temperatures rise [44].

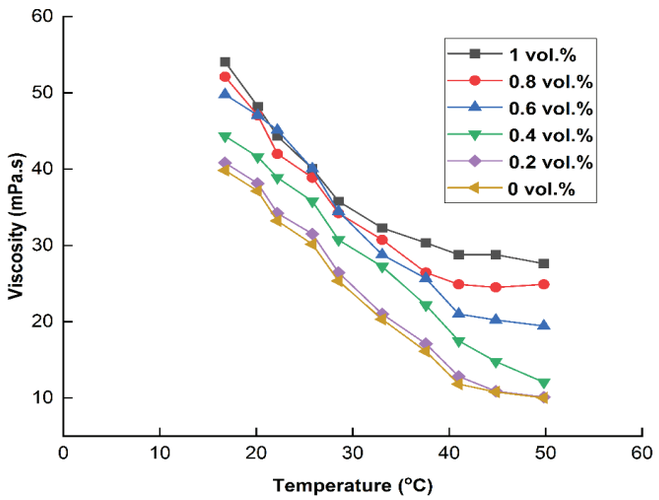

Fig. 11. Al_2O_3 nanofluid vs. temperature for different volume concentrations.

The viscosities of the Al_2O_3-DI water nanofluids at 30°C were calculated and compared to experimental values from the literature. M. Kole, et al. (2010) [45] results on the viscosity of Al_2O_3/DI water were chosen for comparison and are presented in Fig. 12. At 0.2 vol.%, the viscosity of Al_2O_3-DI water nanofluid is the same as that of M. Kole, et al. (2010) [45]. However, the observed viscosity of this study appeared to be greater than that of M. Kole, et al. (2010) [45]. While the nanoparticles and base fluid were the same in both situations, their sources were unique. As a result, variations in the purity and concentrations of the two sources are possible, resulting in this minor discrepancy in viscosity values. Such differences were also observed in other researchers' experimental data for the same nanofluids.

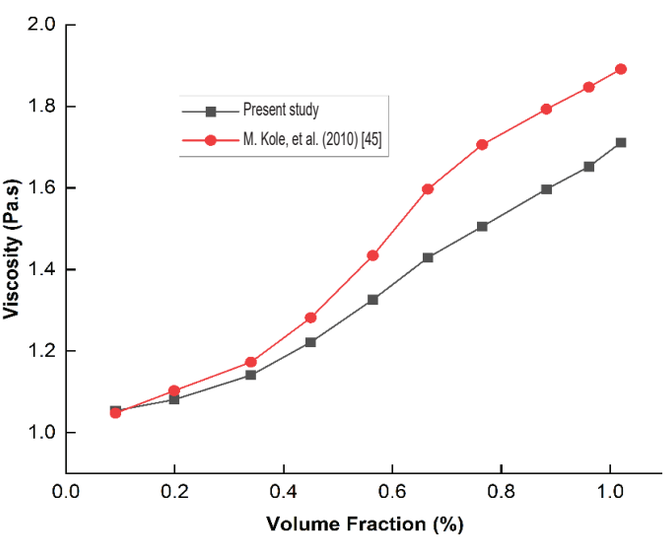

Fig. 12. Model comparison with experimental values [45].

4.4. Comparison of base fluid

To ensure the consistency and precision of the experimental apparatus, preliminary tests were conducted using pure water before proceeding with systematic investigations on the use of nanofluids in the radiator. Fig. 13 presents the experimental findings obtained with a consistent input temperature of 49°C. As anticipated, there is a positive correlation between the Nusselt and Reynolds numbers. Additionally, a comparison was conducted between the experimental results and two established empirical correlations, one proposed [46].

$$N_u = 0.0236 {R_e}^{0.82} {P_r}^{0.3} \quad (8)$$

Figure 13 demonstrates notable concurrence between the Dittus equation and the experimental data within the Reynolds number range employed in this investigation [47]. The findings indicate that the correlation proposed [48] did not align with the current experimental data regarding water flow in flat tubes. The results concerning various water temperatures at the radiator intake, particularly 37, 44, and 49°C, indicate that the Dittus relation exhibits an absolute average inaccuracy of 7%, while the V. Gnielinski's (2009) [48] correlation demonstrates a value of 30% for the exact measurement.

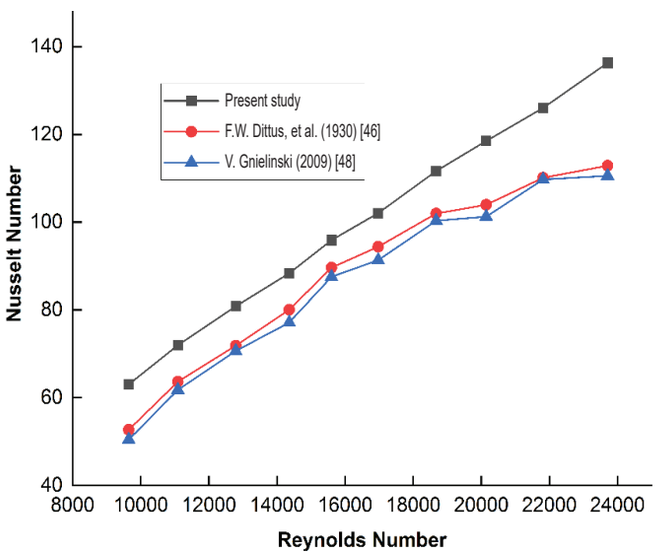

Fig. 13. Experimental results for DI water in comparison with the existing correlations.

5. Conclusions

1. With a nanoparticle concentration of 1 vol.%, the total heat transfer coefficient of Al_2O_3/DI water nanofluids increased by 12% compared to the base fluid.

2. The thermal conductivity of the base fluid was 0.250 W/mK at 10˚C, whereas that of the nanofluid was 0.270 W/mK with a concentration of 1 vol.%, an increase of 8%.

3. The nanofluid's viscosity fell by 61.05% when the temperature was raised from 10 to 50˚C, whereas the viscosity of the base fluid decreased by 72.11% over the same temperature range.

4. The density of Al_2O_3-DI water nanofluid and radiator coolant decreased with increasing temperature, which is connected to the rise in fluid volume caused by increasing temperatures.

Strengths and limitations: It is easy to change the focus on an area and quickly eliminate a lot of heat. Crossflow comprises compressed air to a group of jets that hit a small area. The liquids and air may absorb and transfer heat, but not as effectively as required.

CRediT author statement

M. Peeraiah: Concept, Design, and Data collection; K. Nagamalleswara Rao: Analysis and Interpretation of results; B. Balakrishna: Draft manuscript preparation.

ACKNOWLEDGEMENTS

The authors would like to credit the Dept. of Mechanical Engineering at Sri Venkateshwara College of Engineering, Tirupati, India, for providing testing services used in this study.

COMPETING INTERESTS

The authors declare that there is no conflict of interest regarding the publication of this article.

REFERENCES

[1] A. Kumar, S. Subudhi (2021), *Thermal Characteristics and Convection in Nanofluids*, Springer, DOI: 10.1007/978-981-33-4248-4.

[2] R.G. Naik, A.S. Mohite, F.J. Dadi (2015), "Experimental evaluation of heat transfer rate in automobile cooling system by using nanofluids", *ASME International Mechanical Engineering Congress and Exposition*, 7pp, DOI: 10.1115/IMECE2015-50571.

[3] P.M. Srinivasan, N. Dharmakkan, M.D. Vishnu, et al. (2023), "Heat transfer studies in a plate heat exchanger using Fe_2O_3-water-engine oil nanofluid", *Chemical Industry and Chemical Engineering Quarterly*, **29(3)**, pp.225-233, DOI: 10.2298/CICEQ220430029S.

[4] Z. Said, L.S. Sundar, A.K. Tiwari, et al. (2022), "Recent advances on the fundamental physical phenomena behind stability, dynamic motion, thermophysical properties, heat transport, applications, and challenges of nanofluids", *Physics Reports*, **946**, pp.1-94, DOI: 10.1016/j.physrep.2021.07.002.

[5] A. Kumar, M.A. Hassan, P. Chand (2020), "Heat transport in nanofluid coolant car radiator with louvered fins", *Powder Technology*, **376**, pp.631-642, DOI: 10.1016/j.powtec.2020.08.047.

[6] A. Banisharif, M. Aghajani, S.V. Vaerenbergh, et al. (2020), "Thermophysical properties of water ethylene glycol (WEG) mixture-based Fe_3O_4 nanofluids at low concentration and temperature", *Journal of Molecular Liquids*, **302**, DOI: 10.1016/j.molliq.2020.112606.

[7] Z. Khan, Z.A. Khan, P. Sewell (2019), "Heat transfer evaluation of metal oxides based nano-PCMs for latent heat storage system application", *International Journal of Heat and Mass Transfer*, **144**, DOI: 10.1016/j.ijheatmasstransfer.2019.118619.

[8] I.W. Osho, E.C. Okonkwo, D. Kavaz, et al. (2020), "An experimental investigation into the effect of particle mixture ratio on specific heat capacity and dynamic viscosity of Al_2O_3-ZnO hybrid nanofluids", *Powder Technology*, **363**, pp.699-716, DOI: 10.1016/j.powtec.2020.01.015.

[9] G. Yalçın, S. Öztuna, A.S. Dalkılıç, et al. (2023), "The influence of particle size on the viscosity of water based ZnO nanofluid", *Alexandria Engineering Journal*, **68**, pp.561-576, DOI: 10.1016/j.aej.2022.12.047.

[10] P. Venkataramana, P. Vijayakumar, B. Balakrishna (2022), "Experimental investigation of aluminum oxide nanofluid on closed loop pulsating heat pipe performance", *Journal of Applied Fluid Mechanics*, **15(6)**, pp.1947-1955, DOI: 10.47176/JAFM.15.06.1324.

[11] S. Askari, A. Rashidi, H. Koolivand (2019), "Experimental investigation on the thermal performance of ultra-stable kerosene-based MWCNTs and graphene nanofluids", *International Communications in Heat and Mass Transfer*, **108**, DOI: 10.1016/j.icheatmasstransfer.2019.104334.

[12] M. Jamei, I. Ahmadianfar, I.A. Olumegbon, et al. (2021), "On the assessment of specific heat capacity of nanofluids for solar energy applications: Application of Gaussian process regression (GPR) approach", *Journal of Energy Storage*, **33**, DOI: 10.1016/j.est.2020.102067.

[13] R.S. Vajjha, D.K. Das, D.P. Kulkarni (2010), "Development of new correlations for convective heat transfer and friction factor in turbulent regime for nanofluids", *International Journal of Heat and Mass Transfer*, **53(21-22)**, pp.4607-4618, DOI: 10.1016/j.ijheatmasstransfer.2010.06.032.

[14] J.R. Satti, D.K. Das, D. Ray (2016), "Specific heat measurements of five different propylene glycol based nanofluids and development of a new correlation", *International Journal of Heat and Mass Transfer*, **94**, pp.343-353, DOI: 10.1016/j.ijheatmasstransfer.2015.11.065.

[15] B. Raei, S.M. Peyghambarzadeh (2019), "Measurement of local convective heat transfer coefficient of alumina-water nanofluids in a double tube heat exchanger", *Journal of Chemical and Petroleum Engineering*, **53(1)**, pp.25-36, DOI: 10.22059/jchpe.2019.265521.1247.

[16] M. Zheng, D. Han, F. Asif, et al. (2020), "Effect of Al_2O_3/water nanofluid on heat transfer of turbulent flow in the inner pipe of a double-pipe heat exchanger", *Heat and Mass Transfer*, **56**, pp.1127-1140, DOI: 10.1007/s00231-019-02774-z.

[17] S. Saedodin, M. Zaboli, S.H. Rostamian (2020), "Effect of twisted turbulator and various metal oxide nanofluids on the thermal performance of a straight tube: Numerical study based on experimental data", *Chemical Engineering and Processing - Process Intensification*, **158**, DOI: 10.1016/j.cep.2020.108106.

[18] T.K. Murtadha (2023), "Effect of using Al_2O_3/TiO_2 hybrid nanofluids on improving the photovoltaic performance", *Case Studies in Thermal Engineering*, **47**, DOI: 10.1016/j.csite.2023.103112.

[19] A.H. Pordanjani, S. Aghakhani, M. Afrand, et al. (2019), "An updated review on application of nanofluids in heat exchangers for saving energy", *Energy Conversion and Management*, **198**, DOI: 10.1016/j.enconman.2019.111886.

[20] S. Jena, S.R. Mishra, P.K. Pattnaik (2020), "Development in the heat transfer properties of nanofluid due to the interaction of inclined magnetic field and non-uniform heat source", *Journal of Nanofluids*, **9(3)**, pp.143-151, DOI: 10.1166/jon.2020.1749.

[21] P.K. Pattnaik, D.K. Moapatra, S.R. Mishra (2021), "Influence of velocity slip on the MHD flow of a micropolar fluid over a stretching surface", *Recent Trend in Applied Mathematics: Lecture Notes in Mechanical Engineering*, pp.307-321, DOI: 10.1007/978-981-15-9817-3-21.

[22] S.K. Parida, S. Mishra, R.K. Dash, et al. (2021), "Dynamics of dust particles in a conducting water-based kerosene nanomaterials: A computational approach", *International Journal of Chemical Reactor Engineering*, **19(8)**, pp.787-797, DOI: 10.1515/ijcre-2020-0204.

[23] P.K. Pattnaik, S.K. Parida, S.R. Mishra, et al. (2022a), "Analysis of metallic nanoparticles (Cu, Al_2O_3, and SWCNTs) on magnetohydrodynamics water-based nanofluid through a porous medium", *Journal of Mathematics*, **2022**, pp.1-12, DOI: 10.1155/2022/3237815.

[24] P. Mathur, S.R. Mishra, P.K. Pattnaik, et al. (2021), "Characteristics of Darcy-Forchheimer drag coefficients and velocity slip on the flow of micropolar nanofluid", *Heat Transfer*, **50(7)**, pp.6529-6547, DOI: 10.1002/htj.22191.

[25] P.K. Pattnaik, M.A. Abbas, S. Mishra, et al. (2022b), "Free convective flow of Hamilton-crosser model gold-water nanofluid through a channel with permeable moving walls", *Combinatorial Chemistry & High Throughput Screening*, **25(7)**, pp.1103-1114, DOI: 10.2174/1386207324666210813112323.

[26] P.C. Pattanaik, S.R. Mishra, S. Jena, et al. (2022), "Impact of radiative and dissipative heat on the Williamson nanofluid flow within a parallel channel due to thermal buoyancy", *Proceedings of The Institution of Mechanical Engineers, Part N: Journal of Nanomaterials, Nanoengineering and Nanosystems*, **236(1-2)**, pp.3-18, DOI: 10.1177/23977914221080046.

[27] B. Mohanty, S. Mohanty, S.R. Mishra, et al. (2021), "Analysis of entropy on the peristaltic transport of micropolar nanofluid: A simulation obtained using approximate analytical technique", *The European Physical Journal Plus*, **136**, DOI: 10.1140/epjp/s13360-021-02150-z.

[28] S.R. Mishra, M.M. Hoque, B. Mohanty, et al. (2019), "Heat transfer effect on MHD flow of a micropolar fluid through porous medium with uniform heat source and radiation", *Nonlinear Engineering*, **8(1)**, pp.65-73, DOI: 10.1515/nleng-2017-0126.

[29] S. Baag, S.R. Mishra, M.M. Hoque, et al. (2018), "Magnetohydrodynamic boundary layer flow over an exponentially stretching sheet past a porous medium with uniform heat source", *Journal of Nanofluids*, **7(3)**, pp.570-576, DOI: 10.1166/jon.2018.1478.

[30] B. Nayak, S.R. Mishra, G.G. Krishna (2019), "Chemical reaction effect of an axisymmetric flow over radially stretched sheet", *Propulsion and Power Research*, **8(1)**, pp.79-84, DOI: 10.1016/j.jppr.2019.01.002.

[31] O.D. Makinde, S.R. Mishra (2017), "Chemically reacting MHD mixed convection variable viscosity Blasius flow embedded in a porous medium", *Defect and Diffusion Forum*, **374**, pp.83-91, DOI: 10.4028/www.scientific.net/DDF.374.83.

[32] K.S. Nisar, R. Mohapatra, S.R. Mishra, et al. (2021), "Semi-analytical solution of MHD free convective Jeffrey fluid flow in the presence of heat source and chemical reaction", *Ain Shams Engineering Journal*, **12(1)**, pp.837-845, DOI: 10.1016/j.asej.2020.08.015.

[33] S. Mishra, R.N. Choudhary, S.K. Parida (2022), "Structural, dielectric, electrical and optical properties of Li/Fe modified barium tungstate double perovskite for electronic devices", *Ceramics International*, **48(12)**, pp.17020-17033, DOI: 10.1016/j.ceramint.2022.02.257.

[34] S. Mishra, B. Mahanthesh, J. Mackolil, et al. (2021), "Nonlinear radiation and cross-diffusion effects on the micropolar nanoliquid flow past a stretching sheet with an exponential heat source", *Heat Transfer*, **50(4)**, pp.3530-3546, DOI: 10.1002/htj.22039.

[35] P. Thakur, I. Potoroko, S.S. Sonawane (2022), "Numeric and experimental investigations of performance improvement using nanofluids in car radiators", *Applications of Nanofluids in Chemical and Bio-medical Process Industry*, pp.133-162, DOI: 10.1016/B978-0-323-90564-0.00008-8.

[36] M. Hatami, M. Hasanpour, D. Jing (2020), "Recent developments of nanoparticles additives to the consumables liquids in internal combustion engines: Part III: Nano-coolants", *Journal of Molecular Liquids*, **319**, DOI: 10.1016/j.molliq.2020.114156.

[37] V. Velagapudi, K.R. Konijeti, K.S. Aduru (2008), "Empirical correlations to predict thermophysical and heat transfer characteristics of nanofluids", *Thermal Science*, **12(2)**, pp.27-37, DOI: 10.2298/TSCI0802027V.

[38] Z. Said, N.K. Cakmak, P. Sharma, et al. (2022) "Synthesis, stability, density, viscosity of ethylene glycol-based ternary hybrid nanofluids: Experimental investigations and model-prediction using modern machine learning techniques", *Powder Technology*, **400**, DOI: 10.1016/j.powtec.2022.117190.

[39] A. Ijam, R. Saidur, P. Ganesan, et al. (2015), "Stability, thermo-physical properties, and electrical conductivity of graphene oxide-deionized water/ethylene glycol based nanofluid", *International Journal of Heat and Mass Transfer*, **87**, pp.92-103, DOI: 10.1016/j.ijheatmasstransfer.2015.02.060.

[40] M. Naraki, S.M. Peyghambarzadeh, S.H. Hashemabadi, et al. (2013), "Parametric study of overall heat transfer coefficient of CuO/water nanofluids in a car radiator", *International Journal of Thermal Sciences*, **66**, pp.82-90, DOI: 10.1016/j.ijthermalsci.2012.11.013.

[41] M.M. Elias, I.M. Mahbubul, R. Saidur, et al. (2014), "Experimental investigation on the thermo-physical properties of Al_2O_3 nanoparticles suspended in car radiator coolant", *International Communications in Heat and Mass Transfer*, **54**, pp.48-53, DOI: 10.1016/j.icheatmasstransfer.2014.03.005.

[42] N. Kumar, S.S. Sonawane, S.H. Sonawane (2018), "Experimental study of thermal conductivity, heat transfer and friction factor of Al_2O_3 based nanofluid", *International Communications in Heat and Mass Transfer*, **90**, pp.1-10, DOI: 10.1016/j.icheatmasstransfer.2017.10.001.

[43] R.L. Hamilton, O.K. Crosser (1962), "Thermal conductivity of heterogeneous two-component systems", *Industrial & Engineering Chemistry Fundamentals*, **1(3)**, pp.187-191, DOI: 10.1021/i160003a005.

[44] Z. Said, S. Rahman, P. Sharma, et al. (2022), "Performance characterization of a solar-powered shell and tube heat exchanger utilizing MWCNTs/water-based nanofluids: An experimental, numerical, and artificial intelligence approach", *Applied Thermal Engineering*, **212**, DOI: 10.1016/j.applthermaleng.2022.118633.

[45] M. Kole, T.K. Dey (2010), "Experimental investigation on the thermal conductivity and viscosity of engine coolant based alumina nanofluids", *AIP Conference Proceedings*, **1249(1)**, pp.120-124, DOI: 10.1063/1.3466537.

[46] F.W. Dittus, L.M.K. Boelter (1930), *Heat Transfer in Automobile Radiators of the Tubular Type*, University of California Press, 461pp.

[47] S.M. Peyghambarzadeh, S.H. Hashemabadi, M.S. Jamnani, et al. (2011), "Improving the cooling performance of automobile radiator with Al_2O_3/water nanofluid", *Applied Thermal Engineering*, **31(10)**, pp.1833-1838, DOI: 10.1016/j.applthermaleng.2011.02.029.

[48] V. Gnielinski (2009), "Heat transfer coefficients for turbulent flow in concentric annular ducts", *Heat Transfer Engineering*, **30(6)**, pp.431-436, DOI: 10.1080/01457630802528661.